Please cite this article in press as: Santana et al., Spinal Cord Stimulation Alleviates Motor Deficits in a Primate Model of Parkinson Disease, Neuron (2014), http://dx.doi.org/10.1016/j.neuron.2014.08.061

Neuron
Report

Spinal Cord Stimulation Alleviates Motor Deficits in a Primate Model of Parkinson Disease

Maxwell B. Santana,[1,7,9] Pär Halje,[2,9] Hougelle Simplício,[1,8] Ulrike Richter,[2] Marco Aurelio M. Freire,[1] Per Petersson,[2,10] Romulo Fuentes,[1,10] and Miguel A.L. Nicolelis[1,3,4,5,6,10,*]
[1]Edmond and Lily Safra Institute of Neuroscience of Natal, 590660 Natal, Brazil
[2]Integrative Neurophysiology and Neurotechnology, Neuronano Research Center, Department of Experimental Medical Sciences, Lund University, BMC F10, 221 84 Lund, Sweden
[3]Biomedical Engineering
[4]Center for Neuroengineering
[5]Department of Neurobiology
[6]Department of Psychology and Neuroscience
Duke University, Durham, NC 27708, USA
[7]Psychobiology, Federal University of Rio Grande do Norte, 59072 Natal, Brazil
[8]State University of Rio Grande do Norte, RN 59607-360 Mossoro, Brazil
[9]Co-first author
[10]Co-senior author
*Correspondence: nicoleli@neuro.duke.edu
http://dx.doi.org/10.1016/j.neuron.2014.08.061

SUMMARY

Although deep brain electrical stimulation can alleviate the motor symptoms of Parkinson disease (PD), just a small fraction of patients with PD can take advantage of this procedure due to its invasive nature. A significantly less invasive method—epidural spinal cord stimulation (SCS)—has been suggested as an alternative approach for symptomatic treatment of PD. However, the mechanisms underlying motor improvements through SCS are unknown. Here, we show that SCS reproducibly alleviates motor deficits in a primate model of PD. Simultaneous neuronal recordings from multiple structures of the cortico-basal ganglia-thalamic loop in monkeys with PD revealed abnormal highly synchronized neuronal activity within each of these structures and excessive functional coupling among them. SCS disrupted this pathological circuit behavior in a manner that mimics the effects caused by pharmacological dopamine replacement therapy or deep brain stimulation. These results suggest that SCS should be considered as an additional treatment option for patients with PD.

INTRODUCTION

Chronic electrical stimulation of subcortical brain structures, a procedure known as deep-brain stimulation (DBS), has become an important complement to dopamine replacement therapy in the symptomatic treatment of Parkinson disease (PD) (Benabid et al., 1987). However, partially because of the highly invasive nature of this surgical procedure (Morgante et al., 2007) and its need for additional complex and costly technologies, only a small fraction of all patients with PD who could possibly benefit from this therapy are actually eligible for implantation. In this context, the recent demonstration that electrical epidural spinal cord stimulation (SCS) alleviates akinesia in rodent models of PD (Fuentes et al., 2009) and reduces motor symptoms in patients (Agari and Date, 2012; Fénelon et al., 2012; Hassan et al., 2013; Landi et al., 2012) is a significant finding because SCS, unlike DBS, is minimally invasive. Following the initial report on rodent PD models, SCS has been evaluated for treatment of PD in a few clinical case studies. Results of these studies range from no measurable improvements in two patients (Thevathasan et al., 2010) to significant symptomatic relief (Agari and Date, 2012; Fénelon et al., 2012; Hassan et al., 2013; Landi et al., 2012) in 19 patients. More importantly, in some cases SCS achieved PD symptom relief equivalent to the best effects obtained with pharmacological treatment (Fénelon et al., 2012). At present, the underlying causes for the different outcomes in these preliminary clinical studies are not known, but variations in electrode design, spinal cord implantation location, and choice of stimulation parameters have been suggested as possible contributing factors (Fuentes et al., 2010; Nicolelis et al., 2010). One way to optimize the application of this potential therapy for PD is to establish what neurophysiological changes are associated with the relief of symptoms, and to evaluate how these changes can be most effectively induced. Here, we have addressed these questions by characterizing the behavioral and neurophysiologic SCS effects in 6-OHDA (6-hydroxydopamine) lesioned marmoset monkeys (*Callithrix jacchus*), a primate model of PD.

RESULTS

Using previously described procedures (Annett et al., 1992; Mitchell et al., 1995), five adult male marmosets were caused to be parkinsonian through 6-OHDA stereotactic micro-injections in the medial forebrain bundle of either one (n = 2) or both

hemispheres (n = 3). Injections resulted in neurodegeneration of the midbrain dopaminergic neurons projecting to the forebrain in the lesioned hemispheres, as assessed postmortem through immunohistochemical quantification of tyrosine hydroxylase (Figure S1 available online). In lesioned animals, the number of dopaminergic neurons in the midbrain was reduced to 42% ± 23% of the values observed in control animals. In addition, axonal terminal staining density in the caudate-putamen decreased to 44% ± 10% of the levels seen in normal subjects. The severity of parkinsonism was regularly examined in all marmosets using manual scoring of a wide range of clinical signs/deficits (see Supplemental Experimental Procedures and Movie S1 for details) and automated quantification of spontaneous motor behavior. On average, spontaneous locomotion was reduced to approximately one-fourth of prelesion activity, and PD signs approached the maximum score (mean ± SD: 75% ± 29%) in all the eight categories assessed (Bankiewicz et al., 2001; Verhave et al., 2009).

Once PD clinical signs had been confirmed, animals underwent implantation with bipolar epidural SCS electrodes positioned symmetrically over the dorsal midline of the spinal cord at a high thoracic level (T3–T4). Four of the five animals (two with bilateral and two with unilateral medial forebrain bundle lesions) also underwent chronic implantation with microelectrode arrays/bundles in both hemispheres for subsequent recording of neuronal ensemble activity (both single units and local field potentials [LFPs]; Figure S2). These implants targeted multiple structures in each animal, including the primary motor cortex, putamen, the subthalamic nucleus, globus pallidus pars externa (GPe) and interna, and the ventrolateral and ventral posterolateral thalamic nuclei. In the two unilateral lesion animals, instead of the globus pallidus, parts of primary somatosensory cortex were implanted. Prior to SCS, all animals were also subjected to acute pharmacological inhibition of dopamine synthesis (subcutaneous injections of alpha-methyl-p-tyrosine [AMPT] 2 × 240 mg/kg) to further aggravate the PD signs.

To avoid SCS current intensities that could be experienced as uncomfortable, before each stimulation session the intensity of each stimulation frequency was adjusted and set to 1.7 times the minimum intensity at which any behavioral response could be consistently detected (small postural changes, head or neck movements). Overall, as previously reported in rodents (Fuentes et al., 2009), we observed that SCS induced a clear alleviation of motor impairment in monkeys who exhibited severe clinical PD signs. Because the stimulation frequencies used in this study (range, 4–300 Hz) proved equally effective, the analysis of the SCS effects, both behavioral and electrophysiological, were performed by pooling all the frequencies, unless otherwise stated. All recordings/stimulation sessions were performed in freely behaving animals in a transparent acrylic box. Based on our automated image analysis of digital videos obtained from multiple cameras during neuronal recording sessions, SCS induced a 221% increase in general motility of trunk, head, limbs, and tail ($p < 0.05$, Wilcoxon signed rank test, Figure 1A), a 192% increase in the frequency of bouts of spontaneous locomotion ($p < 0.001$, two-proportional z test, Figure 1B), and a 144% increase in the duration of locomotion periods ($p < 0.05$, Wilcoxon rank sum test, Figure 1C). These improvements resulted in a 243% increase in the total distance covered ($p < 0.05$, Wilcoxon rank sum test, Figure 1D) by the monkeys. Remarkably, SCS induced a preferential increase in the fraction of faster locomotion components, indicating a specific reduction of bradykinesia, ($p < 0.05$, Kolmogorov-Smirnov test of difference in speed histogram distributions, Figure 1E). Overall, the resulting distance covered in locomotive behavior was practically normalized by SCS (on average 91% of intact values, but locomotion differed somewhat in that stimulated animals tended to extend bout duration [628%] whereas reducing the frequency [11%] compared to the intact state). The improvements in motor disability were also assessed by an observer blinded to stimulation conditions that rated specific clinical signs, such as freezing, hypokinesia, bradykinesia, coordination, gait, posture, and gross and fine motor skills, during the OFF and ON periods. The motor deficits that exhibited the highest reduction during SCS were freezing (31%), hypokinesia (23%), posture (23%), and bradykinesia (21%). Overall, the PD score showed, on average, a significant reduction of 18.4% ± 13.9% ($p < 0.001$, Wilcoxon signed rank sum test [including all five subjects], Figure 1F; Figure S1).

In addition to the general clinical improvements observed in all monkeys, in a few instances SCS resulted in an extraordinary functional recovery. An example of this is shown in Figure 1G, where a severely parkinsonian animal, who reached the maximum PD score on all clinical signs rated, showed a dramatic improvement during SCS. This allowed the animal to find and retrieve a food item with no difficulty whatsoever (see Movie S2).

Chronic, multisite neuronal extracellular activity was analyzed both in terms of changes in single neuron's firing patterns and at the level of LFPs. We observed that SCS induced changes in neural populations throughout the cortico-basal ganglia-thalamic loop in parkinsonian animals (Figure 2A). As shown in Figures 2B and 2C, the most noticeable effect was the suppression of LFP power in a frequency interval roughly spanning the beta-band (8–20 Hz), which was abnormally strong in all PD monkeys (respective peak power frequencies for the four subjects were 10, 11, 12, and 15 Hz; Figure S3A; Stein and Bar-Gad, 2013). This suppression of LFP oscillations was observed in all animals and, notably, in all parts of the cortico-basal ganglia-thalamic loop (although it did not reach significance level, $p < 0.05$, in GPe when comparing averaged power spectra; Figures 2B and 2C, $p < 0.05$, Wilcoxon rank sum test on band power 8–20 Hz). In agreement with the behavioral effects, beta suppression could be obtained using both low- and high-frequency SCS paradigms with approximate equal efficacy (average LFP power spectra ON/OFF stimulation for all animals and frequencies are presented in Figure 2B).

Next, we examined the effects of SCS on single unit activity. Overall, approximately one-third of the neurons recorded in the lesioned hemispheres displayed significant changes in firing rates associated with SCS. In contrast to the effect on LFP and motor behavior, SCS modulation of neuronal firing rate differed markedly according to the stimulation frequency (Figure 3A; see also Figure S3C). Whereas stimulation at low frequencies (4–20 Hz) caused mostly excitatory neuronal responses, inhibitory firing modulation predominated during high-frequency stimulation (80–300 Hz; Pearson correlation between the ratio of inhibitory/excitatory responses and stimulation frequency was: primary motor cortex, $r = 0.96$, $p < 0.01$; putamen, $r = 0.74$,

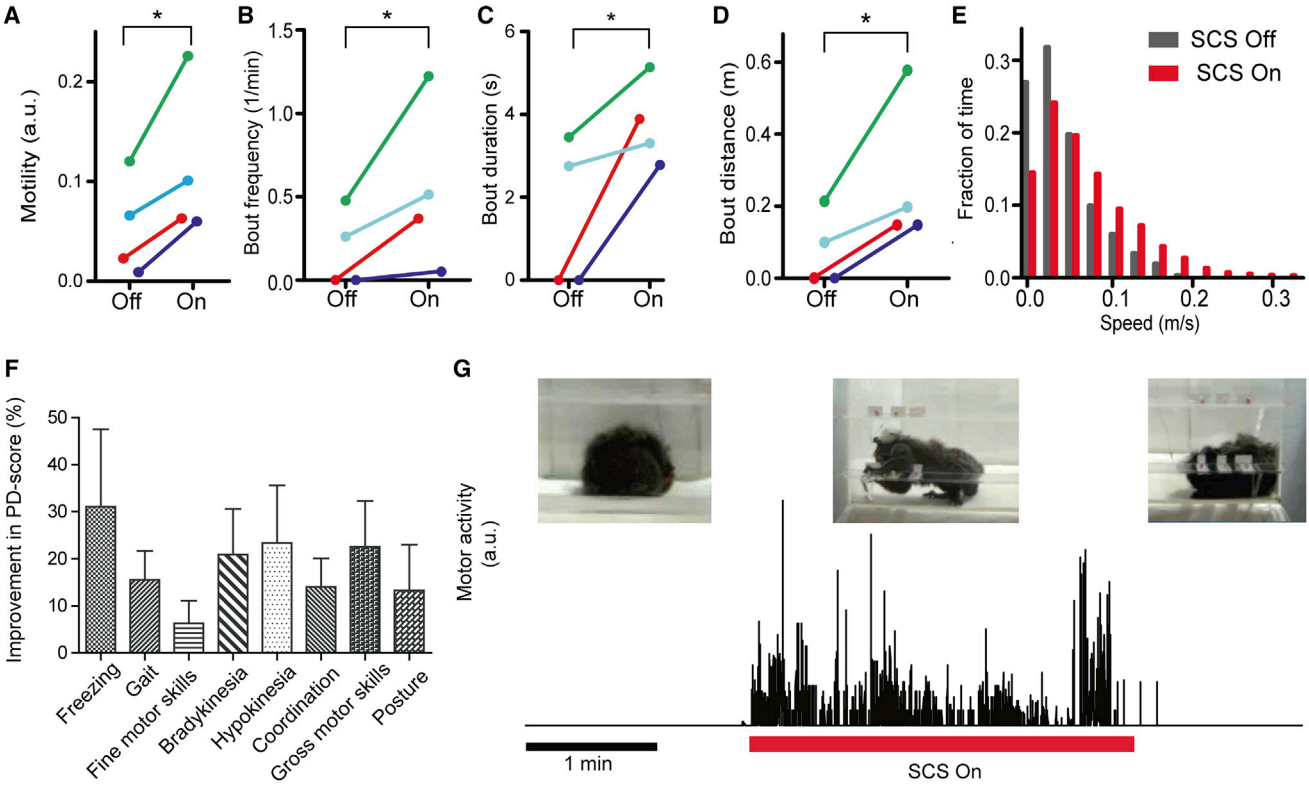

Figure 1. Spinal Cord Stimulation Alleviates Motor Symptoms in Parkinsonian Primates

(A) Average effect on general motility in response to SCS. Each color line represents one recorded animal over all trials.

(B–D) Average recovery of locomotion: bout distance, bout frequency and duration, respectively (colors represent the four different subjects and asterisks denote significant group differences).

(E) Reduction in bradykinesia reflected by the preferential recovery of faster movement components in locomotion.

(F) Average improvements in PD score in all testing sessions divided by symptom category (mean and SEM shown).

(G) Example of functional motor improvement from a state of severe parkinsonism enabling an animal to retrieve food reward using skilled reaching and grasping movements.

$p < 0.05$; ventral posterolateral thalamic nuclei, $r = 0.94$, $p < 0.01$; ventrolateral thalamic nuclei, $r = 0.76$, $p < 0.05$; subthalamic nucleus, $r = 0.92$, $p < 0.01$; GPe and globus pallidus pars interna not significant, Figure 3B).

Consistent with the LFP oscillatory activity, we observed a large fraction of neurons with beta oscillatory firing in the OFF period (Figure 3C) that was partially suppressed during the SCS ON period (Figures 3D, 3E, and S2). In total, 152 of 273 (56%) neurons from the lesioned hemispheres displayed significant beta range (8–16 Hz) rhythmic firing patterns during the OFF periods ($p < 0.01$, as compared to spectra computed from equivalent random spike trains). Of these 152 neurons, 39 (26%) significantly decreased their beta rhythmicity during the SCS ON period. The change in beta power for all units with significant rhythmic activity in the beta range is summarized in Figure 3F.

Taken altogether, these data suggest that SCS-induced motor deficit relief is primarily associated with the disruption of synchronized oscillatory activity rather than with specific changes in firing rate. However, because cortico-basal ganglia activity is known to be strongly influenced by behavioral state, neurophysiologic changes could also result, to some extent, from secondary changes in animal motor behavior. Therefore, to further clarify how SCS induces neurophysiologic changes that may cause symptomatic relief, we compared the neuronal activity patterns from the lesioned hemisphere during SCS, in the two hemilesioned animals, to either the patterns of the intact hemisphere or to the lesioned hemisphere following L-DOPA treatment (subcutaneous 15 mg/kg with benserazide 6.25 mg/kg). Recordings were split into 4 s epochs that were classified as either active or inactive states based on automatically quantified motor activity. To facilitate comparisons between states, two separate indices were constructed. First, two vectors were created summarizing the mean differences (parkinsonian versus intact state) and (parkinsonian versus L-DOPA-treated state), respectively, in two multidimensional parameter spaces—spectral LFP power and firing rate per structure. Each recorded epoch could then be represented as a point in the parameter spaces and be quantitatively compared to the intact or L-DOPA treated state by geometrical projection onto these vectors. Using this metric, it was evident that SCS treatment caused a shift toward healthy brain activity patterns resembling the effect of L-DOPA treatment. This effect was observed only for the analysis of LFP spectral power and not for neuronal firing rates (Figure S3B).

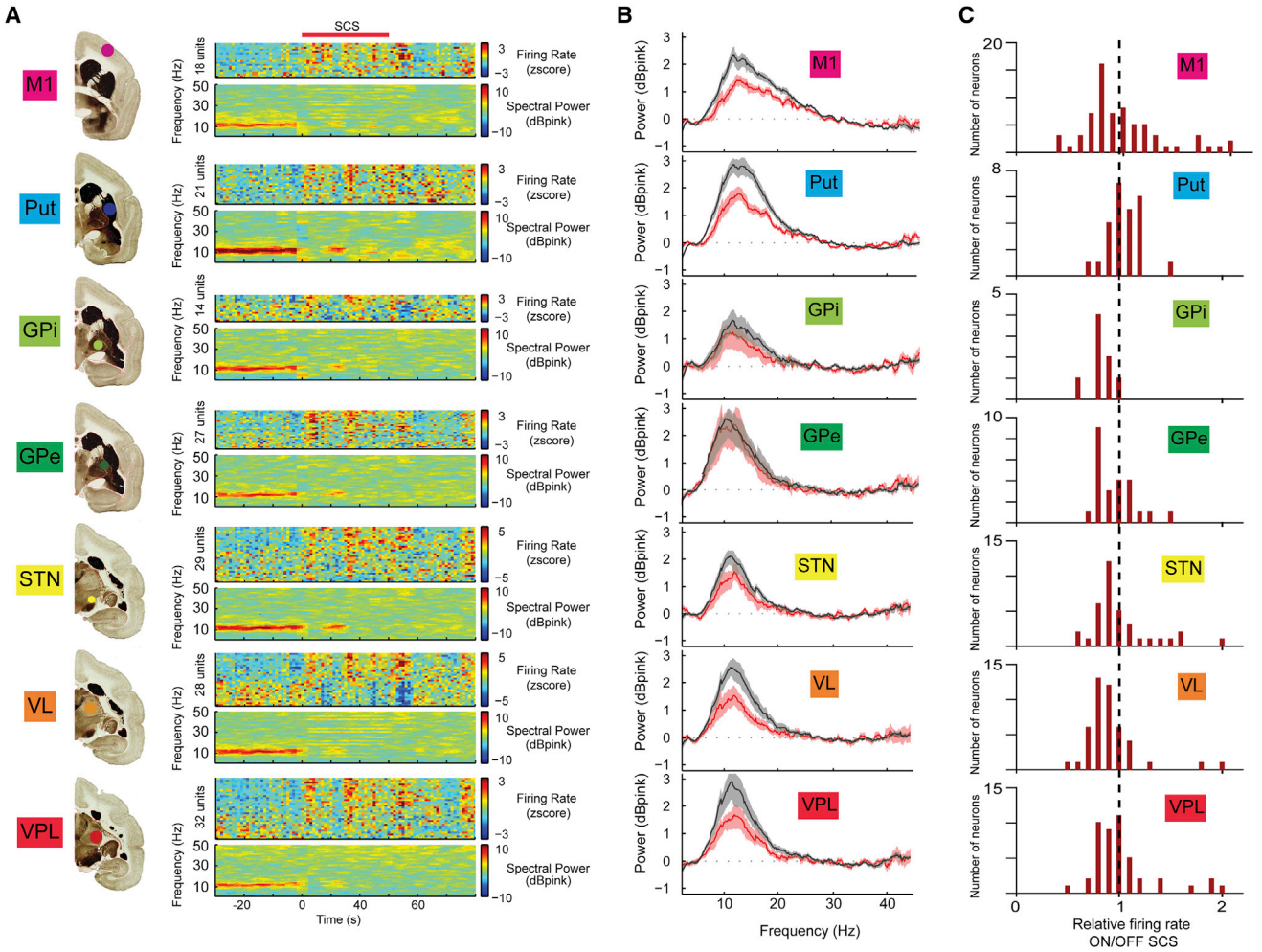

Figure 2. Spinal Cord Stimulation Alters Neuronal Activity Patterns in Basal Ganglia Circuits

(A) Example of parallel changes in LFP power in multiple structures of the cortico-basal ganglia-thalamic loop. For each brain structure, right depicts pooled LFP spectrograms (brain slice figures reproduced with permission from Palazzi andBordier, *The Marmoset Brain in Stereotaxic Coordinates*, Springer Science+-Business Media). Note the immediate reduction of low-frequency oscillations (beta band) in response to SCS (red bar, stimulation frequency: 4 Hz; color codes denote decibels above pink noise background for LFPs).

(B) Average LFP spectra for all recording sessions normalized to pink noise showing a significant SCS-induced reduction in LFP beta-power in all structures except GPe. Shaded area denotes 95% CI with 100 bootstraps.

(C) Changes in normalized firing rates of individual neurons were diverse but, on average, they decreased in response to SCS in globus pallidus pars interna and ventrolateral thalamic nuclei.

Importantly, this shift could not be explained as a secondary effect due to an active or inactive behavioral state because a two-way ANOVA, used to estimate the relative effect size of SCS compared to that of behavioral state, showed that only 2.9% and 0.8% of the total variance (eta-squared; using the metric for the intact and L-DOPA treated state, respectively) could be attributed to behavioral state change, whereas the effect of SCS treatment explained 13.4% and 10.8% of the total variance.

Consequently, the main effect shared by both SCS and L-DOPA treatment appears to be the suppression of the excessive neuronal population synchronization associated with the parkinsonian state. Although it is not clear how coordinated low-frequency activity patterns arise in PD, it is possible that an altered functional coupling between the circuit elements of the cortico-basal ganglia-thalamic loop may be a key underlying factor (Williams et al., 2002). To test this idea, we computed the coherence of the LFP signals between pairs of different neural structures as an indirect measure of their functional connectivity. In the 6-OHDA lesioned dopamine-depleted hemispheres, we found strong coherence between pairs of structures, but only in the parkinsonian low-frequency range (8–15 Hz) (Figure 4A, black traces). Importantly, like the L-DOPA treatment, SCS reduced the beta coherence (Figure 4A red trace), leading to a significant functional decoupling between the different structures. This suggests that SCS brings the functional connectivity of the cortico-basal ganglia-thalamic circuit closer to the normal state of the intact brain. Indeed, this decoupling of parkinsonian LFP oscillations in the beta band was observed between all the recorded

Please cite this article in press as: Santana et al., Spinal Cord Stimulation Alleviates Motor Deficits in a Primate Model of Parkinson Disease, Neuron (2014), http://dx.doi.org/10.1016/j.neuron.2014.08.061

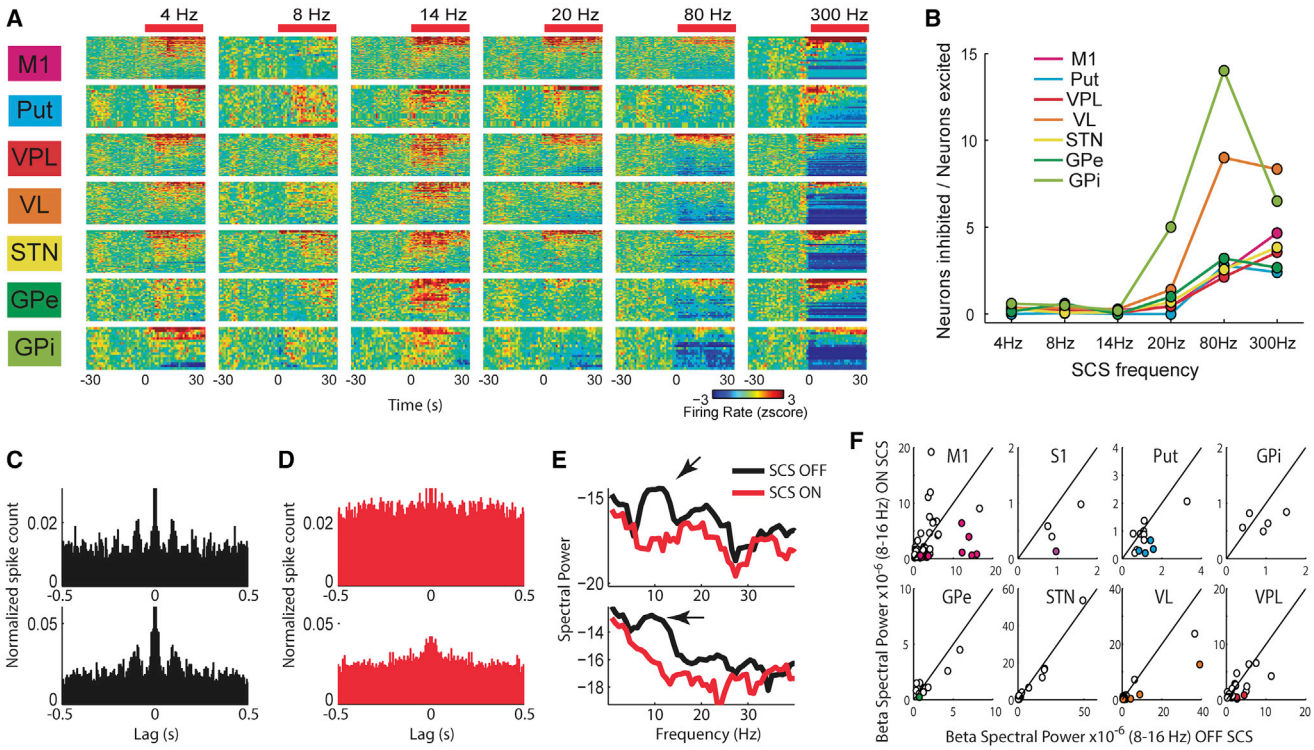

Figure 3. Spinal Cord Stimulation Alters the Firing Rate and Rhythmicity of Neuronal Units in Basal Ganglia Circuits

(A) Standardized neuronal firing rate response to different SCS frequencies in multiple structures of the basal ganglia circuits (neurons rank ordered according to responses).

(B) The fraction of inhibitory responses increased with higher SCS frequencies.

(C) Autocorrelograms of two single units in primary motor cortex exemplifying beta-range rhythmic firing pattern in a parkinsonian animal (SCS OFF).

(D) Autocorrelograms of the same two units showing that the rhythmic spiking is effectively interrupted by SCS.

(E) The respective power spectra OFF/ON (black/red) for the units shown in (C) and (D). Note the peak (arrow) in the beta-range during the OFF period, which disappears during the ON period.

(F) Changes in power of rhythmic beta-firing plotted for all 183 units that presented significant beta oscillations either in the OFF or ON period. Colored circles represent the units with significant suppression in beta power during the ON period. Black line denotes equal power in ON and OFF conditions, thus units located to the right of the line display beta suppression.

structures and was found to be very similar following L-DOPA and SCS (Figure 4B).

To further explore the underlying mechanisms whereby SCS alters network activity, we recorded neural activity while delivering single or pairs of SCS pulses. These recordings showed that primary somatosensory pathways (ventral posterolateral thalamic nuclei and primary somatosensory cortex) are activated early by SCS and that a disruption of beta oscillations through a phase-reset mechanism appears to cause the observed widespread desynchronization in the beta band (Figure S4; Fuentes et al., 2010; Popovych and Tass, 2012).

DISCUSSION

In conclusion, we observed that SCS caused clear clinical improvements in a primate model of PD (comparable to, for example, the reported long-term reduction in UPDRS III score by DBS, ~28%, Follett et al., 2010) and, in particular, for motor signs known to be difficult to treat with DBS. These include deficits in posture, gait, and speed of locomotion (Krack et al., 2003). Concurrent multisite neuronal recordings showed that significant behavioral improvements induced by SCS were strongly associated with desynchronization of neuronal activity within the cortico-basal ganglia circuitry and reduction in beta-frequency coherence between structure pairs. We therefore propose that SCS should be further tested in clinical studies aimed at measuring its long-term efficacy as a less invasive, long-term therapy for patients with PD.

EXPERIMENTAL PROCEDURES

Five adult male common marmosets (*Callithrix jacchus*) 300–550 g were used in the study. The animals were housed in pairs in cages (1.0 × 1.0 × 2.3 m) in a vivarium with a natural light cycle (12/12 hr) and outdoor temperature. All animal procedures were carried out according to approved protocols by AASDAP Ethics Committee and strictly in accordance with the NIH Guide for the Care and Use of Laboratory Animals (NIH Publications no. 80-23). This project was approved by SISBIO/Brazilian Institute of Environment and Natural Resources under no. 20795-2.

Neurotoxic lesions were inflicted with the animals under deep anesthesia. Two microliters of 6-OHDA solution (4 mg/ml, 0.05% ascorbic acid, saline) were injected into the medial forebrain bundle in (AP/ML/DV): 6.5/1.2/6.0;

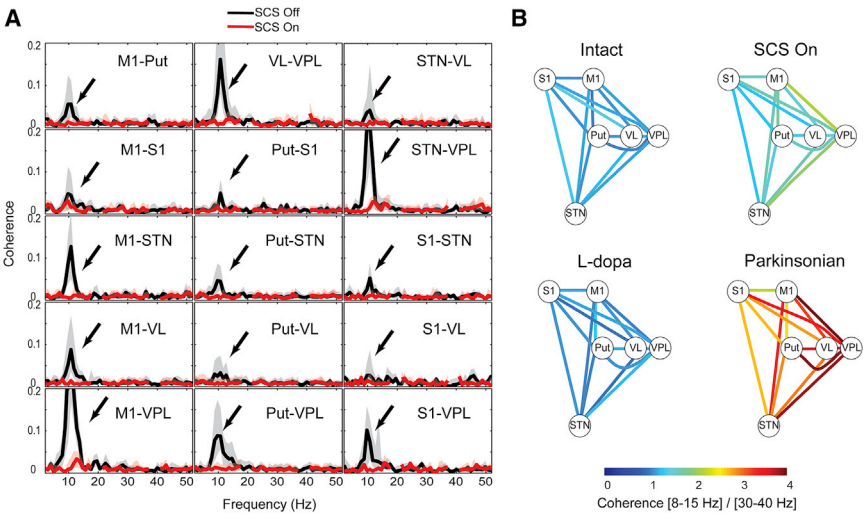

Figure 4. Spinal Cord Stimulation and L-DOPA Treatment Suppresses Multistructure LFP Coherence

(A) Example of LFP coherence spectra from one of the hemilesioned animals (black trace) showing coherent oscillations restricted to the beta-band in the parkinsonian condition (arrows) that are suppressed by SCS (red trace; bold line and shaded area denote median and interquartile range, stimulation artifacts around 20 and 40 Hz have been removed).

(B) Connectivity diagram representing the pooled LFP coherence in the 8–15 Hz range in relation to the 30–40 Hz band between all pairs of electrodes in the different structures (values represent averages from all five recordings in the two hemilesioned animals; all changes in beta-to-gamma coherence for SCS ON/OFF are significant $p < 0.05$, Wilcoxon rank sum test). Note that the excessive beta-band coherence, represented by the warm colors in the parkinsonian state, is effectively reduced by SCS in the same way as for L-DOPA treatment.

6.5/1.2/7.0; 6.5/2.2/6.5; 6.5/2.2/7.5; and 6.5/3.2/8.0 (Annett et al., 1992). AP coordinates were scaled according to the dimensions of the skulls of each animal (Stephan et al., 1980).

The following parkinsonian symptoms were assessed in the transparent acrylic box: episodes of freezing, uncoordinated gait, difficulty using fine motor skills, episodes of bradykinesia, hypokinesia, balance impairment, and posture. The assessment methods were based on previously described procedures (Bankiewicz et al., 2001; Campos-Romo et al., 2009; Fahn and Elton, 1987; Verhave et al., 2009) and are thoroughly described in the Supplemental Experimental Procedures. Automatic motion tracking was performed using custom developed software in MATLAB.

LFPs and action potentials were recorded using a multi-channel recording system (Plexon).

Analyses of recorded signals were performed according to previously described methods (Fuentes et al., 2009; Halje et al., 2012).

The position of the recording electrode positions and the extent of dopaminergic lesions were verified through quantitative tyrosine hydroxylase staining in all animals.

SUPPLEMENTAL INFORMATION

Supplemental Information includes Supplemental Experimental Procedures, four figures, and two movies and can be found with this article online at http://dx.doi.org/10.1016/j.neuron.2014.08.061.

AUTHOR CONTRIBUTIONS

M.S, H.S, P.H., R.F, P.P, and M.A.L.N. designed the experiments; M.S, H.S, R.F., and P.P performed the surgeries; M.S. conducted experiments; M.S. and M.F. performed immunohistochemistry; M.S., P.H., U.R., P.P., R.F., and M.A.L.N. analyzed the data, and M.S., P.H, U.R, P.P., R.F., and M.A.L.N. wrote the paper.

ACKNOWLEDGMENTS

We thank Tobias Palmér for developing the video tracking software used for automatic quantification of locomotor behavior, Jim Meloy and Gary Lehew for building recording electrodes, Ivani Brys for statistical discussion, Carlos Eduardo Idalino for support with data analysis, Pedro Calvacanti for support in IHC, and Marcelo Carvalho for technical support. This research was supported by The Michael J. Fox Foundation for Parkinson's Research; FINEP 01.06.1092.00; INCEMAQ—Program of National Institutes of Science and Technology of CNPq/MCT; the Swedish Research Council (325-2011-6441); Swedish Society for Medical Research; the Olle Engkvist, Parkinson Research, Crafoord, Åke Wiberg, Magnus Bergvall, Kockska and Segerfalk Foundation; and an NIH Transformative award (R01-NS073125-03).

Accepted: August 28, 2014
Published: October 30, 2014

REFERENCES

Agari, T., and Date, I. (2012). Spinal cord stimulation for the treatment of abnormal posture and gait disorder in patients with Parkinson's disease. Neurol. Med. Chir. (Tokyo) *52*, 470–474.

Annett, L.E., Rogers, D.C., Hernandez, T.D., and Dunnett, S.B. (1992). Behavioural analysis of unilateral monoamine depletion in the marmoset. Brain *115* (Pt 3), 825–856.

Bankiewicz, K.S., Sanchez-Pernaute, R., Oiwa, Y., Kohutnicka, M., Cummins, A., and Eberling, J. (2001). Preclinical models of Parkinson's disease. In Current Protocols in Neuroscience (John Wiley & Sons), pp. 9.4.1–9.4.32.

Benabid, A.L., Pollak, P., Louveau, A., Henry, S., and de Rougemont, J. (1987). Combined (thalamotomy and stimulation) stereotactic surgery of the VIM thalamic nucleus for bilateral Parkinson disease. Appl. Neurophysiol. *50*, 344–346.

Campos-Romo, A., Ojeda-Flores, R., Moreno-Briseño, P., and Fernandez-Ruiz, J. (2009). Quantitative evaluation of MPTP-treated nonhuman parkinsonian primates in the HALLWAY task. J. Neurosci. Methods *177*, 361–368.

Fahn, S., and Elton, R.L. (1987). Unified Parkinson's disease rating scale. Recent Dev. Park. Dis. *2*, 153–163.

Fénelon, G., Goujon, C., Gurruchaga, J.-M., Cesaro, P., Jarraya, B., Palfi, S., and Lefaucheur, J.-P. (2012). Spinal cord stimulation for chronic pain improved motor function in a patient with Parkinson's disease. Parkinsonism Relat. Disord. *18*, 213–214.

Follett, K.A., Weaver, F.M., Stern, M., Hur, K., Harris, C.L., Luo, P., Marks, W.J., Jr., Rothlind, J., Sagher, O., Moy, C., et al.; CSP 468 Study Group (2010). Pallidal versus subthalamic deep-brain stimulation for Parkinson's disease. N. Engl. J. Med. *362*, 2077–2091.

Fuentes, R., Petersson, P., Siesser, W.B., Caron, M.G., and Nicolelis, M.A.L. (2009). Spinal cord stimulation restores locomotion in animal models of Parkinson's disease. Science *323*, 1578–1582.

Fuentes, R., Petersson, P., and Nicolelis, M.A. (2010). Restoration of locomotive function in Parkinson's disease by spinal cord stimulation: mechanistic approach. Eur. J. Neurosci. *32*, 1100–1108.

Halje, P., Tamtè, M., Richter, U., Mohammed, M., Cenci, M.A., and Petersson, P. (2012). Levodopa-induced dyskinesia is strongly associated with resonant cortical oscillations. J. Neurosci. *32*, 16541–16551.

Hassan, S., Amer, S., Alwaki, A., and Elborno, A. (2013). A patient with Parkinson's disease benefits from spinal cord stimulation. J. Clin. Neurosci. *20*, 1155–1156.

Krack, P., Batir, A., Van Blercom, N., Chabardes, S., Fraix, V., Ardouin, C., Koudsie, A., Limousin, P.D., Benazzouz, A., LeBas, J.F., et al. (2003). Five-year follow-up of bilateral stimulation of the subthalamic nucleus in advanced Parkinson's disease. N. Engl. J. Med. *349*, 1925–1934.

Landi, A., Trezza, A., Pirillo, D., Vimercati, A., Antonini, A., and Sganzerla, E.P. (2012). Spinal cord stimulation for the treatment of sensory symptoms in advanced Parkinson's disease. Neuromodulation *16*, 276–279.

Mitchell, I.J., Hughes, N., Carroll, C.B., and Brotchie, J.M. (1995). Reversal of parkinsonian symptoms by intrastriatal and systemic manipulations of excitatory amino acid and dopamine transmission in the bilateral 6-OHDA lesioned marmoset. Behav. Pharmacol. *6*, 492–507.

Morgante, L., Morgante, F., Moro, E., Epifanio, A., Girlanda, P., Ragonese, P., Antonini, A., Barone, P., Bonuccelli, U., Contarino, M.F., et al. (2007). How many parkinsonian patients are suitable candidates for deep brain stimulation of subthalamic nucleus? Results of a questionnaire. Parkinsonism Relat. Disord. *13*, 528–531.

Nicolelis, M.A., Fuentes, R., Petersson, P., Thevathasan, W., and Brown, P. (2010). Spinal cord stimulation failed to relieve akinesia or restore locomotion in Parkinson disease. Neurology *75*, 1484, author reply 1484–1485.

Popovych, O.V., and Tass, P.A. (2012). Desynchronizing electrical and sensory coordinated reset neuromodulation. Front. Hum. Neurosci. *6*, 58.

Stein, E., and Bar-Gad, I. (2013). β oscillations in the cortico-basal ganglia loop during parkinsonism. Exp. Neurol. *245*, 52–59.

Stephan, H., Baron, G., and Schwerdtfeger, W.K. (1980). The Brain of the Common Marmoset (Callithrix jacchus) : A Stereotaxic Atlas. (New York: Springer).

Thevathasan, W., Mazzone, P., Jha, A., Djamshidian, A., Dileone, M., Di Lazzaro, V., and Brown, P. (2010). Spinal cord stimulation failed to relieve akinesia or restore locomotion in Parkinson disease. Neurology *74*, 1325–1327.

Verhave, P.S., Vanwersch, R.A., van Helden, H.P.M., Smit, A.B., and Philippens, I.H.C.H.M. (2009). Two new test methods to quantify motor deficits in a marmoset model for Parkinson's disease. Behav. Brain Res. *200*, 214–219.

Williams, D., Tijssen, M., Van Bruggen, G., Bosch, A., Insola, A., Di Lazzaro, V., Mazzone, P., Oliviero, A., Quartarone, A., Speelman, H., and Brown, P. (2002). Dopamine-dependent changes in the functional connectivity between basal ganglia and cerebral cortex in humans. Brain *125*, 1558–1569.